**Ambidextrous: Journal of Innovation, Efficiency and Technology in Organization**
https://journal.takaza.id/index.php/ambidextrous
Vol. 4, No. 04, 2026, pp. 292-298
E-ISSN: 3031-7002
E-mail:ambidex@takaza.id



# Sensitivity of Water Saturation to Formation Water Resistivity in Argillaceous Sandstone

**Muhammad Alghifari***
Program Studi Teknik Produksi Minyak dan Gas, Politeknik Energi dan Mineral Akamigas, Cepu, Indonesia
Corresponding Author e-mail:alghi100103@gmail.com

**Article History:**
Received : 03-11-2026
Revised : 12-11-2026
Accepted : 19-11-2026

**Keywords:** ***Sensitivity Analysis; Argillaceous Sandstone; Formation Water Resistivity; Water Saturation; Simandoux***

***Abstract:*** *Formation water resistivity (Rw) is a major source of uncertainty in water saturation (Sw) calculations, particularly when formation water samples and clean water zones are unavailable. This study evaluates the sensitivity of Sw to Rw in argillaceous sandstones of the Petani Formation, Central Sumatra Basin, at depths of 1,358 and 1,359 ft in Well A, Field X. A quantitative sensitivity analysis was conducted using the Larionov equation for old rocks to estimate shale volume, shale-corrected neutron-density logs to calculate effective porosity, and the generalized Simandoux equation solved iteratively (a = 1.65; m = 1.8; n = 1.8). Sw was evaluated across an Rw range of 0.01–0.40 ohm-m and compared with four reference values: apparent water resistivity (Rwa), software-generated Rw, critical Rw, and implicit Rw. Both intervals exhibit low shale volume (0.056–0.072) and high effective porosity (0.335–0.345). However, Sw varies substantially with Rw, and both intervals meet the Sw cut-off of 0.60 only when Rw is ≤0.062–0.068 ohm-m, approximately half the Rwa values (0.121–0.122 ohm-m). The software-generated Rw values (0.335–0.348 ohm-m) produce calculated Sw values greater than 1, indicating mathematically inconsistent results rather than physically acceptable water saturation. Meanwhile, reproducing the software-generated Sw values requires implicit Rw values approximately nine times lower. These findings demonstrate that uncertainty in Rw can substantially alter reservoir prospectivity interpretation. Therefore, independent Rw determination is essential before classifying the analyzed intervals as prospective hydrocarbon zones.*

**How to Cite:** Muhammad Alghifari. (2026). Sensitivity of Water Saturation to Formation Water Resistivity in Argillaceous Sandstone. *4*(04). Pp.292-298. https://doi.org/10.61536/ambidextrous.v4i04.1003

https://doi.org/10.61536/ambidextrous.v4i04.1003

This is an open-access article under theCC-BY-SA License.

## Introduction

Water saturation (Sw) is the most important determinant in assessing a prospective zone, as the in-place hydrocarbon volume is calculated directly from the pore fraction that does not contain water. From log data, Sw is derived through the relationship between formation resistivity, porosity, and formation water resistivity (Rw) formulated by Archie (1942). These three inputs are not equivalent. Formation resistivity and porosity are available at every depth from the log curve, while Rw is a fluid property that must be determined from other sources (Bassiouni, 1994; Ellis & Singer, 2007).

In practice, Rw can be obtained from laboratory analysis of formation water samples, from the deflection of the spontaneous potential curve, from the apparent water resistivity (Rwa) in the water-saturated zone, or from a Pickett plot that utilizes the distribution of points in the water zone (Pickett, 1966; Asquith & Krygowski, 2004). Each method has prerequisites, such as the availability of a clean sandstone layer that can be confirmed to contain water. If these prerequisites are not met, the interpreter must choose Rw based on assumptions, and such choices can shift Sw significantly without being visible in the final results.

Difficulties arise in shaly sandstones. Clay minerals also conduct electricity, so the Archie equation tends to overestimate Sw. Various models have been developed to correct for this effect, including Simandoux (1963), Waxman and Smits (1968), the Indonesian equation (Poupon & Leveaux, 1971), and the dual-water model (Clavier et al., 1984); a review of their development is presented by Worthington (1985). Nevertheless, Rw remains a major multiplier in these models. Incorrect determination of Rw in low-resistivity reservoirs can lead to the overestimation of hydrocarbon reservoirs or, conversely, the underestimation of water reservoirs (Worthington, 2000). Similar uncertainties also exist in the Archie constants a, m, and n, which are ideally determined from laboratory testing of rock core samples (Tiab & Donaldson, 2015).

The Petani Formation in the Central Sumatra Basin represents an environment where both of these uncertainties can coexist. This Late Miocene–Pliocene formation is composed of shale and mudstone intercalated with younger, less-compacted sandstones (Heidrick & Aulia, 1993). In Well A of Field X, petrophysical software output identified the sandstone at 1,358–1,359 ft as a prospective zone, but the parameters underlying this assessment are undocumented.

Rather than establishing a single correct Rw value, this study treats Rw as a variable. The goal is to measure the sensitivity of Sw to Rw at both points, determine the Rw threshold that makes this interval pass or fail the prospect criteria, and assess the consistency of the software's Rw with the calculated results.

## Research Methods

Data are from a single open-hole well, referred to in this article as Well A in Field X; the original well and field names have been replaced with codes to protect the confidentiality of the data owner. The analysis focused on two points in the upper Petani Formation (Petani A), 1358 and 1359 ft, chosen because of their low and uniform gamma ray response and their density–neutron crossover, which is indicative of light hydrocarbons (Rider & Kennedy, 2011). The curves used include gamma ray, deep laterolog resistivity as an approximation of true formation resistivity (Rt), bulk density, density correction (Δρ), neutron porosity, and caliper. For comparison, Rw and Sw values from commercial petrophysical software are available, but without access to the parameter panel. The calculation parameters are summarized in Table 1.


https://doi.org/10.61536/ambidextrous.v4i04.1003
This open-access article is distributed under a Creative Commons Attribution (CC-BY-SA) 4.0 license

**Table 1.Calculation parameters**

| Parameter | Symbol | Mark |
|---|---|---|
| GR clean sandstone; GR shale (API) | GRmin; GRmax | 50.57; 222.84 |
| Matrix density; fluid; shale (g/cc) | ρma; ρf; ρsh | 2.65; 1.0; 2.27 |
| Shale neutron porosity (v/v) | ΦN,sh | 0.607 |
| Shale resistivity (ohm-m) | Rsh | 0.212 |
| Tortuosity factor; cementation exponent; saturation exponent | *a*; M N | 1.65; 1.8; 1.8 |
| *Cut-off*Vsh; Φe; Sw | – | ≤ 0.40; ≥ 0.10; ≤ 0.60 |

The values of a, m, and n in Table 1 are the interpretation parameters used in processing this well data. The gamma ray index is calculated using equation (1) and converted to shale volume using Larionov's (1969) equation for old rocks (2). This equation provides the largest Vsh among the common empirical equations, so the resulting shale correction is conservative.

$$IGR = \frac{GR - GR_{min}}{GR_{max} - GR_{min}} \quad (1)$$

$$V_{sh} = 0{,}33(2^{2 \cdot IGR} - 1) \quad (2)$$

Density porosity is calculated using equation (3). Neutron and density porosity are then corrected for shale content using equations (4) and (5), with shale density porosity from equation (6). Both are then combined into effective porosity through the root mean square (7), which is appropriate for zones with light hydrocarbon hints (Asquith & Krygowski, 2004).

$$\Phi_D = \frac{\rho_{ma} - \rho_b}{\rho_{ma} - \rho_f} \quad (3)$$

$$\Phi_{N,c} = \Phi_N - V_{sh} \cdot \Phi_{N,sh} \quad (4)$$

$$\Phi_{D,c} = \Phi_D - V_{sh} \cdot \Phi_{D,sh} \quad (5)$$

$$\Phi_{D,sh} = \frac{\rho_{ma} - \rho_{sh}}{\rho_{ma} - \rho_f} \quad (6)$$

$$\Phi_e = \sqrt{\frac{\Phi_{N,c}^2 + \Phi_{D,c}^2}{2}} \quad (7)$$

The apparent water resistivity is calculated by assuming the point under consideration is completely filled with water (8). Water saturation is calculated using the Archie equation (9) as a comparison and the general form of the Simandoux equation (10) as the main model.

$$R_{wa} = \frac{R_t \cdot {\Phi_e}^m}{a} \quad (8)$$

$$S_w = \left(\frac{a \cdot R_w}{{\Phi_e}^m \cdot R_t}\right)^{1/n} \quad (9)$$

$$\frac{1}{R_t} = \frac{{\Phi_e}^m \cdot {S_w}^n}{a \cdot R_w} + \frac{V_{sh} \cdot S_w}{R_{sh}} \quad (10)$$

The often-cited direct solution form of the Simandoux equation is only valid for n = 2. Since this study uses n = 1.8, equation (10) is solved iteratively using the bisection method until the difference between the two sides is less than 10−6; in Microsoft Excel, the equivalent steps can be performed using the Goal Seek feature.

For the sensitivity analysis, Sw was calculated over the Rw range of 0.01–0.40 ohm-m at each point. Four reference values were marked on the resulting curve: Rwa from equation (8), which in the hydrocarbon zone is the upper limit of the actual Rw; the Rw recorded in the software output; the critical


https://doi.org/10.61536/ambidextrous.v4i04.1003
This open-access article is distributed under a Creative Commons Attribution (CC-BY-SA) 4.0 license

Rw, which is the value that produces an Sw of exactly 0.60; and the implicit Rw, which is the value required by equation (10) to make Sw equal to the software output. The latter two values were obtained by solving equation (10) with respect to Rw. To check whether the difference in Rw can be explained by the difference in reference temperature, the Arps (1953) relationship with temperature in °F was used:

$$R_{w2} = R_{w1} \cdot \frac{T_1 + 6{,}77}{T_2 + 6{,}77} \tag{11}$$

As a secondary comparison, the sensitivity of Sw to the choice of the Vsh equation was tested by replacing the Larionov equation of the older rocks with the Larionov equation of the Tertiary rocks.

**Results and Discussion**

The analyzed interval is located in the hole widening zone, with a caliper reading of 11.8 inches against an 8.5-inch bit size. However, the density corrections at both points are only −0.016 and −0.009 g/cc, or less than one-third of the commonly used 0.05 g/cc threshold, so the density tool pad contact is considered good. Figure 1 shows the log curves around this interval, including the density–neutron crossover at 1356–1358 ft and a nearly constant software Sw of 0.47.

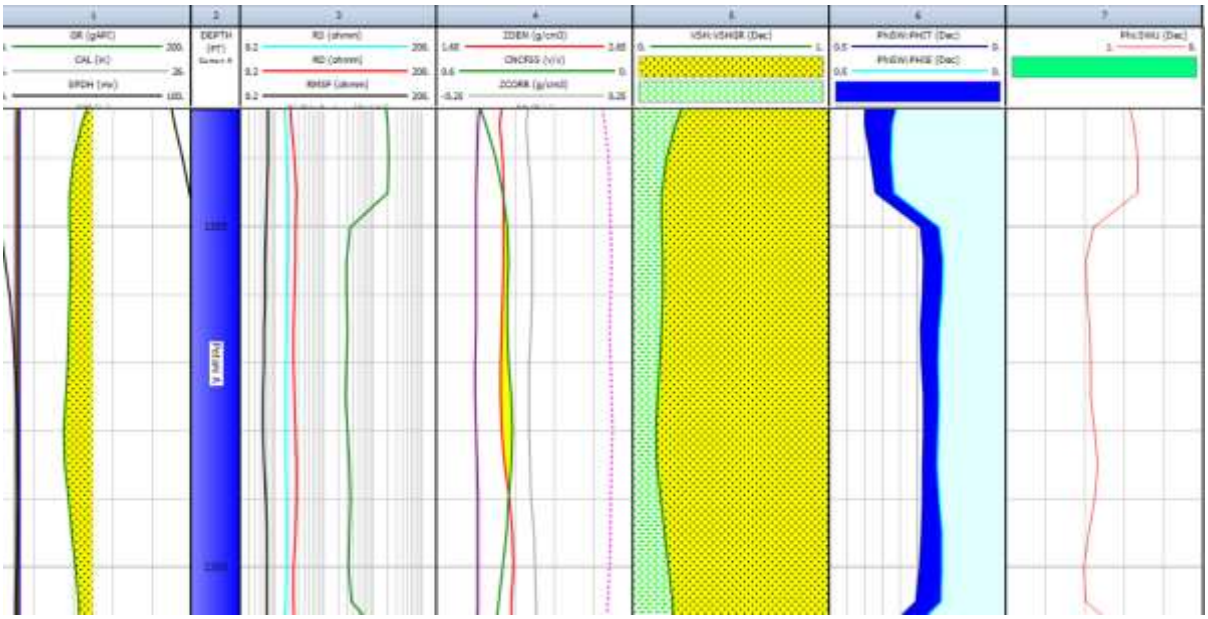


**Figure 1.Log curve and software output at approximately 1355–1360 ft depth, Well A**

**Table 2.Input data and rock properties**

| Depth (ft) | GR (API) | Rt (ohm-m) | ρb (g/cc) | ΦN | Vsh | ΦN,c | ΦD,c | Φe |
|---|---|---|---|---|---|---|---|---|
| 1358 | 70 | 1.37 | 1,980 | 0.322 | 0.056 | 0.288 | 0.393 | 0.345 |
| 1359 | 75 | 1.43 | 2,018 | 0.343 | 0.072 | 0.300 | 0.367 | 0.335 |

Table 2 shows that both points have low shale content (Vsh 0.056–0.072) and high effective porosity (0.335–0.345), far beyond the Vsh and Φe cut-off limits. At both points, ΦD,c exceeds ΦN,c, in line with the crossover in Figure 1. From the rock perspective, both are good reservoirs, so their prospect status depends entirely on Sw.

With a = 1.65 and m = 1.8, the formation factor is 11.22 at 1358 ft and 11.83 at 1359 ft, giving Rwa of 0.122 and 0.121 ohm-m, respectively. The closeness of these two values indicates similar fluid character. However, since both points are suspected to contain hydrocarbons, Rwa can only be treated as an upper limit: the actual Rw must be equal to or less than this value. It should also be noted that if


https://doi.org/10.61536/ambidextrous.v4i04.1003
This open-access article is distributed under a Creative Commons Attribution (CC-BY-SA) 4.0 license

Rwa is re-inserted as Rw into the Archie equation, the result is always Sw = 1, since equation (8) is simply equation (9) inverted with Sw = 1. In the Simandoux equation, the obtained Sw (0.822 and 0.772) are below 1 solely because of the shale term, which under these conditions contributes about 30–37% of the total conductivity. These values are therefore upper limits on Sw, not estimates of saturation in their own right.

Figure 2 presents Sw as a function of Rw at both points, while Table 3 summarizes Sw at the four reference values. Both curves rise sharply at low Rw and flatten at high Rw. Over the range tested, Simandoux's Sw ranges from approximately 0.24 to over 1.2. In other words, a point at the same depth can be considered either a hydrocarbon zone or a water zone simply because of differences in Rw.

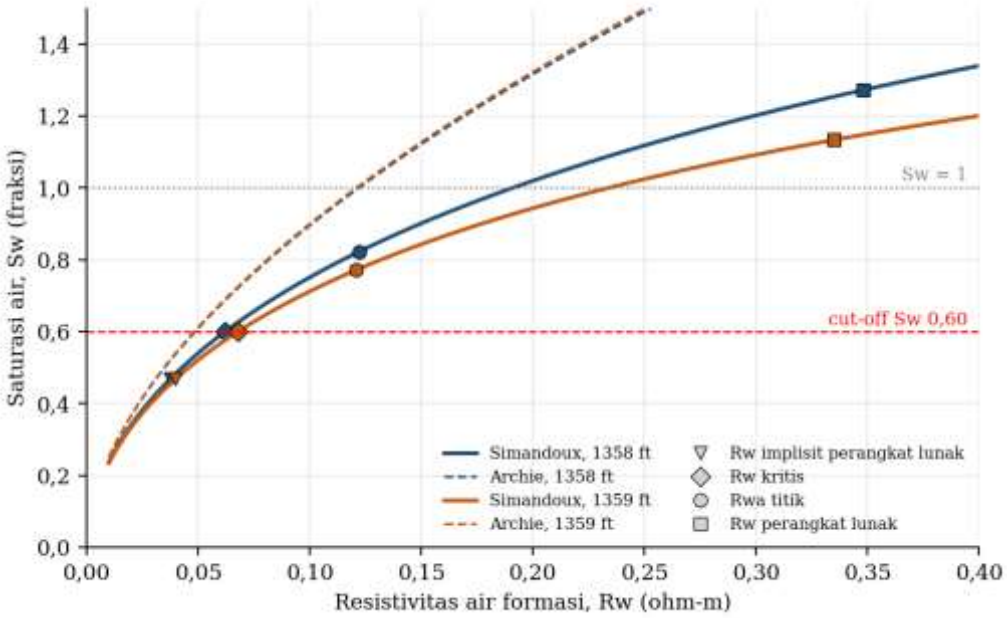



**Figure 2.Sensitivity curve of Sw against Rw at depths of 1358 and 1359 ft**

**Table 3.Water saturation at four reference Rw values**

| Rw Scenario | Rw 1358 ft (ohm-m) | Sw Simandoux | Sw Archie | Rw 1359 ft (ohm-m) | Sw Simandoux | Sw Archie |
|---|---|---|---|---|---|---|
| Implicit Rw | 0.038 | 0.469 | 0.520 | 0.040 | 0.468 | 0.540 |
| Critical RW | 0.062 | 0.600 | 0.687 | 0.068 | 0.600 | 0.726 |
| Rwa point | 0.122 | 0.822 | 1,000 | 0.121 | 0.772 | 1,000 |
| Rw software | 0.348 | 1,272 | 1,790 | 0.335 | 1,134 | 1,762 |

The critical Rw is 0.062 ohm-m at 1358 ft and 0.068 ohm-m at 1359 ft. This means that both points can only be considered prospective if the actual Rw is no more than approximately half of Rwa. Since Rwa is only an upper limit, this possibility is open, but cannot be proven from the available log data. The prospect status of this interval ultimately depends on one question: whether the Rw of the Petani Formation at this location is below approximately 0.06–0.07 ohm-m.

The software output Rw (0.348 and 0.335 ohm-m) are nearly three times Rwa. Since Rwa is already an upper limit, these values are not physically consistent with the log data, and when inserted into equation (10) yield Sw of 1.272 and 1.134. In contrast, the software Sw (0.469 and 0.468) can only be recovered with implicit Rw of 0.038 and 0.040 ohm-m, or 8.4–9.3 times lower than the recorded Rw. The most frequently proposed explanation for such discrepancies is differences in reference temperature, since water resistivity decreases as temperature increases. However, assuming the software Rw is


https://doi.org/10.61536/ambidextrous.v4i04.1003
This open-access article is distributed under a Creative Commons Attribution (CC-BY-SA) 4.0 license

recorded at 75 °F, equation (11) shows that a decrease of 8–9 times would require a formation temperature of about 680–750 °F, an impossible figure for a depth of about 1360 ft. The discrepancy is more likely due to the software's different Archie constants, saturation models, or porosity definitions. This cannot be confirmed without access to the parameter panel, but it is sufficient to suggest that the Rw values in the software output cannot be interpreted independently of the other parameters.

The dashed line in Figure 2 shows Archie's Sw, which is consistently higher than Simandoux's Sw. The critical Rw according to Archie is only 0.048–0.049 ohm-m, so the shale correction widens the Rw tolerance by 28–41%. Although the Vsh at both points is small, the low resistivity of shale (0.212 ohm-m) makes the shale term still significant. On the other hand, the choice of the Vsh equation is much less influential. At Rw = Rwa, replacing the older Larionov with the Tertiary Larionov decreases Vsh to 0.028–0.036 and increases Sw to 0.906 and 0.874, respectively, or shifts of about 0.08–0.10. These shifts are small compared to the 0.36–0.45 change in Sw between the Rwa and software Rw scenarios, so in this interval Rw is the primary source of uncertainty and Vsh is only a secondary source.

These findings should be read in conjunction with their limitations. The analysis covers only two points in a single interval, the constants a, m, and n were not derived from laboratory tests, a software parameter panel is not available, and there are no rock core samples or bed flow tests to compare Sw.

## Conclusion and Suggestions

The Petani Formation sandstone at 1358 and 1359 ft in Well A of Field X is of good reservoir quality, with Vsh of 0.056–0.072 and Φe of 0.335–0.345. However, the Sw of both points is very sensitive to Rw: within a reasonable range of Rw, the assessment can shift from the hydrocarbon zone to the water zone. Both points only meet the Sw cut-off of 0.60 when Rw ≤ 0.062–0.068 ohm-m, approximately half the Rwa upper limit of Rw (0.121–0.122 ohm-m). The software-generated Rw is inconsistent with the log data, producing Sw > 1, while the software-generated Sw can only be recovered with Rw approximately nine times smaller, a difference that cannot be explained by temperature correction alone. The effect of Rw on Sw also far outweighs the effect of the choice of the Vsh equation.

Based on these findings, log interpreters and field decision-makers are advised not to designate the 1358–1359 ft interval as a prospect zone until Rw has been independently obtained, for example through analysis of formation water samples, spontaneous potential curves supplemented with mud filtrate resistivity and formation temperature data, or Pickett plots in thicker water zones. Users of petrophysical software are also advised to always document the constants and models used along with the interpretation results. Further research should expand the number of analysis points and validate the results with rock core data or layer flow tests.

## Thank-you note

The authors would like to thank the data providers and field supervisors for permission to use the data, as well as the lecturers of the Oil and Gas Production Engineering Study Program, Akamigas Energy and Mineral Polytechnic, for their guidance during the research.

## Bibliography

Archie, G. E. (1942). The electrical resistivity log as an aid in determining some reservoir characteristics. *Transactions of the AIME, 146*(1), 54–62. https://doi.org/10.2118/942054-G

Arps, J. J. (1953). The effect of temperature on the density and electrical resistivity of sodium chloride solutions. *Journal of Petroleum Technology, 5*(10), 17–20.

Asquith, G., & Krygowski, D. (2004). *Basic well log analysis* (2nd ed.). American Association of Petroleum Geologists.

Bassiouni, Z. (1994). *Theory, measurement, and interpretation of well logs*. Society of Petroleum


https://doi.org/10.61536/ambidextrous.v4i04.1003
This open-access article is distributed under a Creative Commons Attribution (CC-BY-SA) 4.0 license

Engineers.
Clavier, C., Coates, G., & Dumanoir, J. (1984). Theoretical and experimental bases for the dual-water model for interpretation of shaly sands. *Society of Petroleum Engineers Journal*, *24*(2), 153–168.
Ellis, D. V., & Singer, J. M. (2007). *Well logging for earth scientists* (2nd ed.). Springer.
Heidrick, T. L., & Aulia, K. (1993). A structural and tectonic model of the Coastal Plains Block, Central Sumatra Basin, Indonesia. *Proceedings of the Indonesian Petroleum Association 22nd Annual Convention*, 285–317.
Larionov, V. V. (1969). *Borehole radiometry*. Nedra.
Pickett, G. R. (1966). A review of current techniques for determination of water saturation from logs. *Journal of Petroleum Technology*, *18*(11), 1425–1433.
Poupon, A., & Leveaux, J. (1971). Evaluation of water saturation in shaly formations. *SPWLA 12th Annual Logging Symposium*.
Rider, M., & Kennedy, M. (2011). *The geological interpretation of well logs* (3rd ed.). Rider-French Consulting.
Simandoux, P. (1963). Dielectric measurements on porous media: Application to the measurement of water saturations: Study of the behaviour of argillaceous formations. *Revue de l'Institut Français du Pétrole*, *18*(Suppl.), 193–215.
Tiab, D., & Donaldson, E. C. (2015). *Petrophysics: Theory and practice of measuring reservoir rock and fluid transport properties* (4th ed.). Gulf Professional Publishing.
Waxman, M. H., & Smits, L. J. M. (1968). Electrical conductivities in oil-bearing shaly sands. *Society of Petroleum Engineers Journal*, *8*(2), 107–122.
Worthington, P. F. (1985). The evolution of shaly-sand concepts in reservoir evaluation. *The Log Analyst*, *26*(1), 23–40.
Worthington, P. F. (2000). Recognition and evaluation of low-resistivity pay. *Petroleum Geoscience*, *6*(1), 77–92.


https://doi.org/10.61536/ambidextrous.v4i04.1003
This open-access article is distributed under a Creative Commons Attribution (CC-BY-SA) 4.0 license